

FACE DETECTION IN INFRARED SPECTRUM

by

Nikhil Mahajan

A THESIS

Submitted to the Faculty of Stevens Institute of Technology
in partial fulfillment of the requirements for the degree of

MASTER OF ENGINEERING – ELECTRICAL

Nikhil Mahajan, Candidate

ADVISORY COMMITTEE

Hong Man, Advisor Date

Yu-Dong Yao, Reader Date

STEVENS INSTITUTE OF TECHNOLOGY
Castle Point on Hudson
Hoboken, NJ 07030
2014

FACE DETECTION IN INFRARED SPECTRUM

ABSTRACT

In recent years, Biometrics has received unprecedented attention for verification and authenticity and face recognition is an intriguing area domain for recognizing human patterns. This paper presents an easier approach to detect human face in thermal imaging, which is instrumental towards deleterious effects of the variable light. Also, the scale invariant feature extraction has been applied. It has plethora of properties to be suitable for different images of an object or scene to sub-pixel accuracy well localized in both spatial and frequency domain properties.

Author: Nikhil Mahajan

Advisor: Prof. Hong Man

Date: December 14, 2014

Department: Electrical and Computer Engineering

Degree: Master of Engineering

Acknowledgements

I would like to express my sincere gratitude to my master thesis advisor, Dr. Hong, Man for the useful comments, remarks and engagement through the learning process of this master thesis. Furthermore, I would like to thank Dr. A., Abhyankar for introducing me to the world of Image and Video Processing. Last, but not the least my wonderful parents and my friends, who have supported me through the entire process, both by keeping me harmonious and helping me putting pieces together.

Table of Contents

Abstract	ii
Acknowledgements	iii
List of Figures	iv
Chapter 1: Introduction	1
Chapter 2: Literature Review	5
Chapter 3: Head Curve Geometry based Face Detection	23
Chapter 4: Image matching using Scale Invariant Feature Transform	36
Chapter 5: Conclusion and Future Scope	40
References	42

List of Figures

Figure 1. Radiation spectrum ranges.

Figure 2. Generic map of superficial blood vessels on the face.

Figure 3. Flowchart of feature extraction algorithm.

Figure 4. Convolution of variable scale Gaussian.

Figure 5. Function to detect stable keypoint locations.

Figure 6. Scale normalized laplacian of gausiisan.

Figure 7. Octave of scale space.

Figure 8. Maxima and minima of the difference of Gaussian images.

Figure 9. Frequency of sampling in the spatial domain.

Figure 10. Keypoints location detected in transformed images.

Figure 11. Determine the interpolated location of the maximum.

Figure 12. Stages of keypoint selection.

Figure 13. Function for derivative extremum.

Figure 14. Function value at derivative extremum.

Figure 15. Hessian matrix and eigenvalues.

Figure 16. Function to check principal curvature.

Figure 17. Function to derive orientation histogram.

Figure 18. Orientation assignment of keypoints.

Figure 19. Image gradients and keypoint descriptors.

Figure 20. Probability of match in keypoint matching.

Figure 21. SIFT matching on different faces.

Figure 22. SIFT workflow.

Figure 23. Thermal imaging based face detection system.

Figure 24. Back camera interface, FLIR A20M.

Figure 25. Experimental setup of thermal camera.

Figure 26. Flowchart of proposed algorithm.

Figure 27. Input & extracted red component image.

Figure 28. Morphological operations.

Figure 29. Image with extracted boundary.

Figure 30. Plot of various points on the head.

Figure 31. Curve plot on the head boundary.

Figure 32. Face separated image using head curve geometry.

Figure 33. Reference image & Image with descriptors.

Figure 34. Matched points in reference image.

Figure 35. Pose estimation.

Figure 36. Pyramid plots for reference and current image.

Chapter 1

Introduction

In recent years, Biometrics [1], the ability to distinguish individuals diversely and relate human characteristics and traits (name, nationality, color etc.) with their physiological and behavioral attributes has gained unprecedented attention from both academic and business communities. Personal identification [2], the process of associating a particular individual with an identity has forayed from traditional fingerprint analysis to iris and retina recognition, behavioral patterns, body temperature, signatures, hand analysis etc. Though analysis has vacillating results, the surge in the identity theft crisis specially related to web based services e.g., online banking, and credit card frauds have heightened concerns regarding reliability of systems to verify the authenticity of an individual.

Matters like national security viz. money laundering, human trafficking etc. also have roots in the insecure environment. Recognizing human face is an intriguing domain to identify the human behavioral patterns. A widely accepted mode of identification, it is unobtrusive and challenging [3]. Human face has lineage of many biometric traits acquired over millions of years which sets apart an individual from another in terms of DNA variability or the visible patterns of lines drawn on head or hands for the instant. From the perspective of computer vision,

the field that relates high dimensional data acquired from the real world to numerical or symbolic information, these traits can be utilized for identification or authentication or to classify individual characteristics for swift recognition in environments where security is a major concern by processing the image data through many statistical computations. For example, Personal computers, Sony PlayStation has the ability to let the user access the system after capturing the face through a camera and verifying from pre available data stored in memory.

Research in face domain is primarily biased towards the visible spectrum [4] academically and commercially, undeniably because of availability of low cost visible band cameras. They seem to be a seemingly effortless choice, but the conventional digital images suffer from erratic lightning conditions because of the reflective nature of incident light in the visible spectrum. Environmental darkness may not only degrade picture quality, in turn lowers the output performance too. Secondary problems associate with the cryptic facial cover-ups [5].

Near-infrared imagery for face recognition has been tested with positive results [6]. Since infrared like visible images originates from the reflected radiations, an external illumination source is essential. The blessing over the traditional process is eye not being sensitive to IR range and illumination is more flexible and implemented in a covert manner. As a solution to the above problem [7], researchers have started considering the thermal infrared images as an apt

choice for the face recognition [8]. Despite the fact inquisition in thermal imaging is instrumental towards the deleterious effects of variable light [9] either to reduce darkness or to enhance visibility in the dark [10]. This approach doesn't differ much from the algorithms implemented in visible band based classified as appearance based [11] or feature based [12]. To amalgamate [13] the visible and infrared modalities [14] for performance enhancements [15] attempts have been made in recent past.

For facial recognition algorithms like HAAR [16], Support Vector Machines [17] (SVM), Neural Networks [18] have been in existence but they are statistically complex and time consuming with extra time required for sub-sampling and training. This paper implements a slightly modified approach of *Face detection in thermal imaging using Head Curve Geometry by W.K. Wong, J.H. Hui* [19] for segmenting face from the rest of the body for further processing.

The detected output face is further processed using the Scale Invariant Feature Transform [20] to detect and describe scale, transformation and rotation invariant features in the images. Preceding chapters discuss more about the Head Curve Geometry and implementation of SIFT algorithm for matching similar feature points on two images, and perform a least square pose estimation for the location of the image within the current image.

The chapters include the literature review, algorithms implemented and result along with the conclusion and future scope for this work in Infrared domain. The list of papers and all other references can be found in Bibliography.

Chapter 2

Literature Review

Burgeoning awareness in the security and privacy domain has pressed people to sway away from traditional forms of authentication viz. Magnetic ID Cards, time-variant RSA algorithms etc. Also they have not been able to meet present needs and therefore, biometrics has gained much attention and importance in recent times. Biometrics boasts comparison of physical characteristics or the personal traits in the available database to determine the authenticity of an individual. Physical identity is necessarily for strict confirmations using fingerprints, retinal scan, facial features etc., while most commonly used personal traits, signature and sound veins [21] are convenient in general but less secure and may differ drastically solely for recognition purposes.

For biometric authentication, face recognition has received unprecedented interests recently due to advances in technology [22], and research work in Eigen faces [23] along with the noticeable increase in concerns linked to security [24]. Numerous approaches like ear image [25], gait analysis [26] exists for use primarily in the public spaces. Thermal imaging has been widely implemented in industries for detection of faults of operating systems or line components. Furthermore, this technique is extended to personal identification and recognition

for e.g. anxiety detection, security screening at airports, banks etc., and measuring body temperatures for medical purposes.

A thermal infrared camera with good sensitivity process images with more precision and provide better output results for the recognition purposes [27] and also indirect the superficial blood vessel on the human face [28]. Blood flow causes local variations in the skin temperature, prominently observable on the human face where the layer of flesh is very thin. Human face and body emit both the mid (3-5 μm) and far infrared (8-12 μm) bands, which sense the temperature distributions at a distance to produce 2D images.

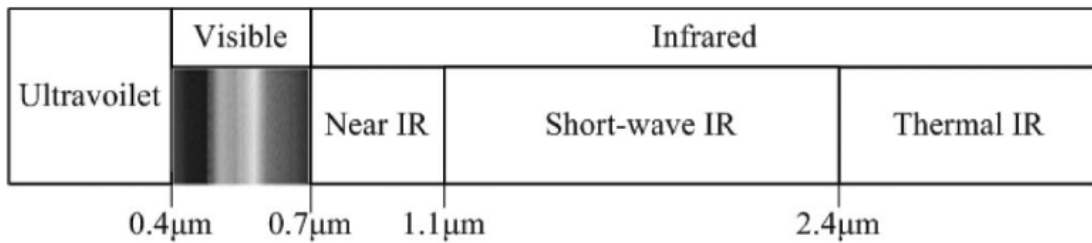


Figure 1. Radiation spectrum ranges. Reference [29]

Various algorithms like HAAR; Voila Jones can be used to determine size, shape and locations of human faces in digital images. Eigen faces, Support Vector Machines, Artificial Neural Networks are famous post-processing image algorithms, but are time consuming and statistically complex. In this paper have tried to implement a much easier & faster algorithm, which are statistically less

complex and yields faster computational results without any hassles of training and sub sampling. Method has been detailed in the preceding chapter. Resultant output image is further processed using Scale Invariant Feature Transform (SIFT) for template matching.

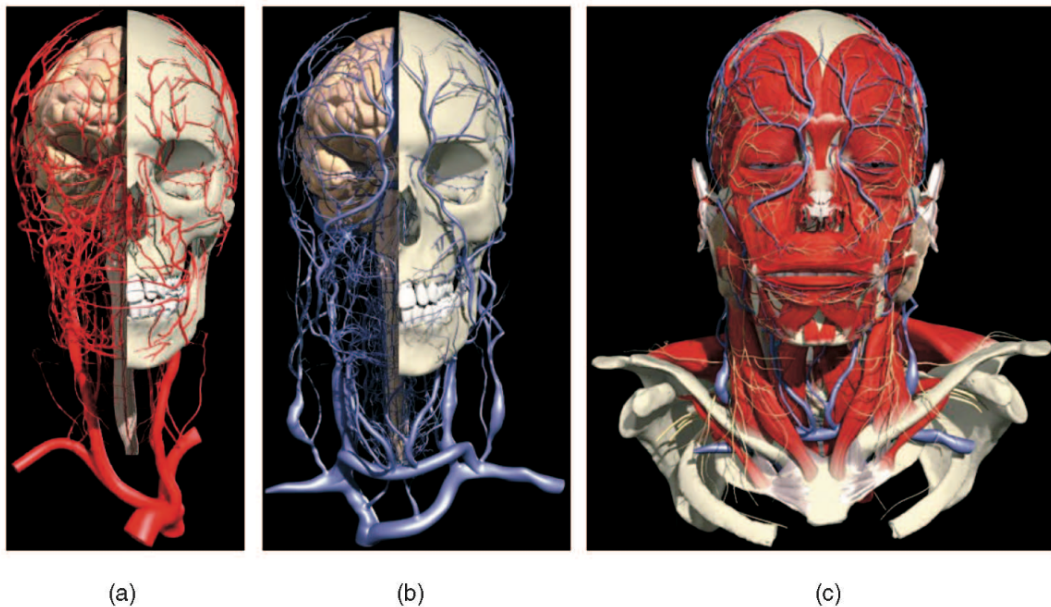


Figure 2. Generic map of superficial blood vessels on the face [30] a) Overview of an arterial network b) Overview of a venous network c) Arteries and veins together underneath the surface of the facial skin.

2.1 Scale Invariant Feature Extraction

Image Matching [31] a key area in image analysis and processing and computer vision is widely used in areas such as industrial inspection, terrain analysis,

medical diagnosis, military applications, image retrieval, object or scene recognition, solving for 3D structure from multiple images, stereo correspondence and motion tracking. The features that have a plethora of properties to be a match for different images of an object or scene to sub-pixel accuracy are well localized in spatial and frequency domains [32].

Since, the features are highly distinctive for a single feature to be correctly matched in the large database of features with a higher probability. This forms basis for the object and scene recognition. Implementing cascade-filtering approach minimizes the cost of extracting features those passes the initial tests. The major stages of computation [33] used to generate the set of image features.

1. Scale-space extrema detection: The difference of Gaussian function is implemented over all scales and image locations to identify potential interest points that are invariant to scale and orientation.
2. Key point Localization: Key points are selected based on measures of their stability at each candidate location.
3. Orientation assignment: The invariance transformations are performed on an image that has been transformed relative to the assigned location for each feature.

4. Keypoint Descriptor: The local image gradients are transformed into a representation that allows for significant levels of local shape distortion and change in illumination. X

This approach has been named Scale Invariant Feature Transform, as it transforms image data into scale-invariant coordinates relative to local features. Feature parameters detect smaller objects explicitly in the cluttered background. Three features must be correctly matched from each object for reliable identification. Therefore, it is an expansive term for a precise matching of an object.

The basic morphological operations dilation and erosion are performed convolving the structuring element (SE) with the image [34]. Other operations include opening, closing or top-hat operation [35]. For image matching and recognition, SIFT features are first extracted from a set of reference image and later stored in a database.

The following figure 3 shows the algorithm for feature extraction.



Figure 3. Flowchart: Feature Extraction Algorithm.

The new image is matched by comparing each feature of the new image to the previous in database based on the Euclidean distance of the feature vectors. The highly distinctive keypoint descriptors allows single feature to seek correct matches. In cluttered images, the false alarms can be eradicated by identifying subsets of keypoints based on the object and its location, scale and orientation in the new image. Consistent clusters can be determined using an efficient hash table implementation of the generalized Hough transform [36], a popular robust method for detecting lines in an image that are extended to identify positions of arbitrary shapes, most commonly circle or ellipses [37].

2.1.1 Detection of scale space extrema

A continuous function of scale known as space scale [38] is implemented by searching for stable features, across all possible scales in an image. This is defined as a function, $L(x,y,\sigma)$, obtained from the convolution of a variable scale Gaussian $G(x,y,\sigma)$, with an input image, $I(x,y)$:

$$L(x, y, \sigma) = G(x, y, \sigma) * I(x, y),$$

Where * is the convolution operation in x and y, and

$$G(x, y, \sigma) = \frac{1}{2\pi\sigma^2} e^{-(x^2+y^2)/2\sigma^2}.$$

Figure 4. Convolution of variable scale Gaussian. Reference [32]

The difference of two nearby scales separated by a constant multiplicative factor k computes the Gaussian function convolved with the image D(x,y,σ).

$$\begin{aligned} D(x, y, \sigma) &= (G(x, y, k\sigma) - G(x, y, \sigma)) * I(x, y) \\ &= L(x, y, k\sigma) - L(x, y, \sigma). \end{aligned}$$

Figure 5. Function to detect stable keypoint locations. Reference [32]

An efficient approach for construction of D(x,y,σ), is shown above in figure 6. The scale normalized Laplacian of Gaussian [39] can $\sigma^2 \nabla^2 G$ is computed as,

$$\sigma \nabla^2 G = \frac{\partial G}{\partial \sigma} \approx \frac{G(x, y, k\sigma) - G(x, y, \sigma)}{k\sigma - \sigma}$$

And therefore,

$$G(x, y, k\sigma) - G(x, y, \sigma) \approx (k - 1)\sigma^2 \nabla^2 G.$$

Figure 6. Scale Normalized Laplacian of Gaussian. Reference [32]

The Gaussian function incorporates the σ^2 scale normalization for the scale-invariant Laplacian. The factor $(k-1)$ remains constant over all scales, and approximation error will go to zero as k goes to 1.

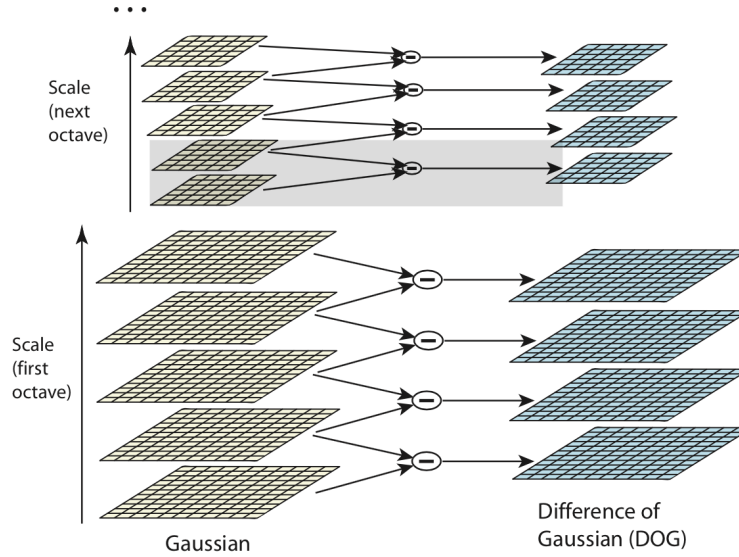


Figure 7. For each octave of scale space, the initial image is repeatedly convolved with Gaussians to produce the set of scale space images shown on the left. Adjacent Gaussian images are subtracted to produce the difference of Gaussian images on the right. After each octave the Gaussian image is down sampled by a factor of 2, and the process repeated. Reference [32]

2.1.1.1 Local Extrema Detection

In order to determine the local maxima and minima of $D(x,y,\sigma)$, each sample point is compared to its neighboring elements as shown in figure 8. The cost of

this check is reasonably low due to the fact that most sample points will be eliminated following the first check.

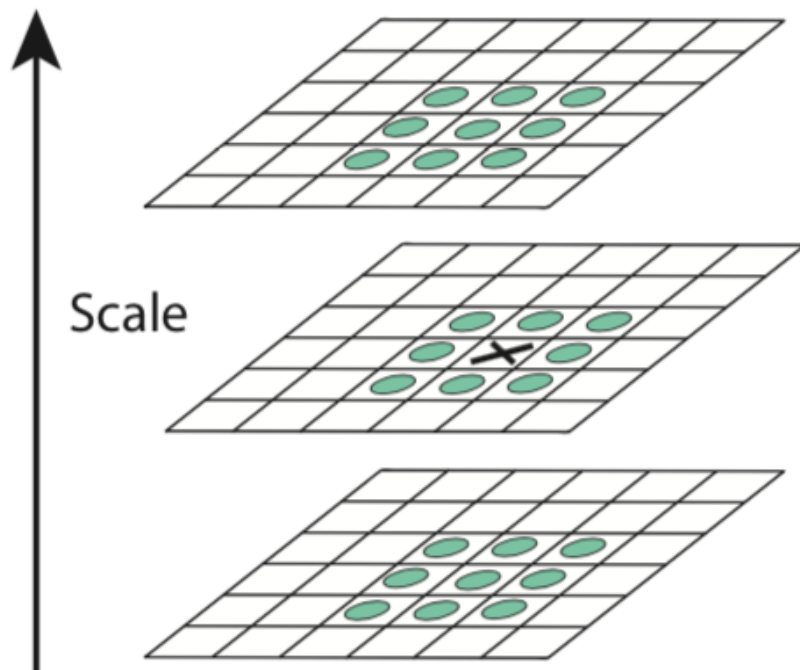


Figure 8. Maxima and minima of the difference of Gaussian images are detected by marking a pixel (X) to its neighbors (O) at the current and adjacent scale.

Reference [32]

2.1.1.2 Frequency of Sampling in scale

Figure 9 shows the experimental determination of sampling frequency that maximizes extrema stability.

2.1.1.3 Frequency of sampling in the spatial domain

Figure 10 shows the frequency of sampling in the image domain relative to the smoothing scale.

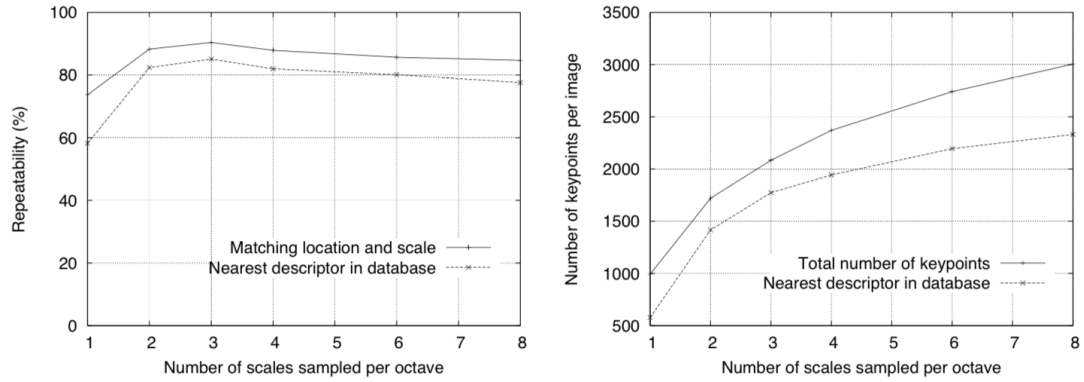


Figure 9. The top line of first graph shows the percent of key points that are reputably detected at the same location and lower line shows the percent of key points that have their descriptors perfectly matched to a large database. The second graph shows the total number of key points detected in a typical image.

Reference [32]

2.1.2 Accurate keypoint localization

Compare neighboring pixels with found keypoint candidate to perform a detailed fit on the nearby data for location, scale, and ratio of principal curvatures. The

function $D(x,y,\sigma)$, is expanded [40] using the Taylor Expansion, for origin to be at the sample point.

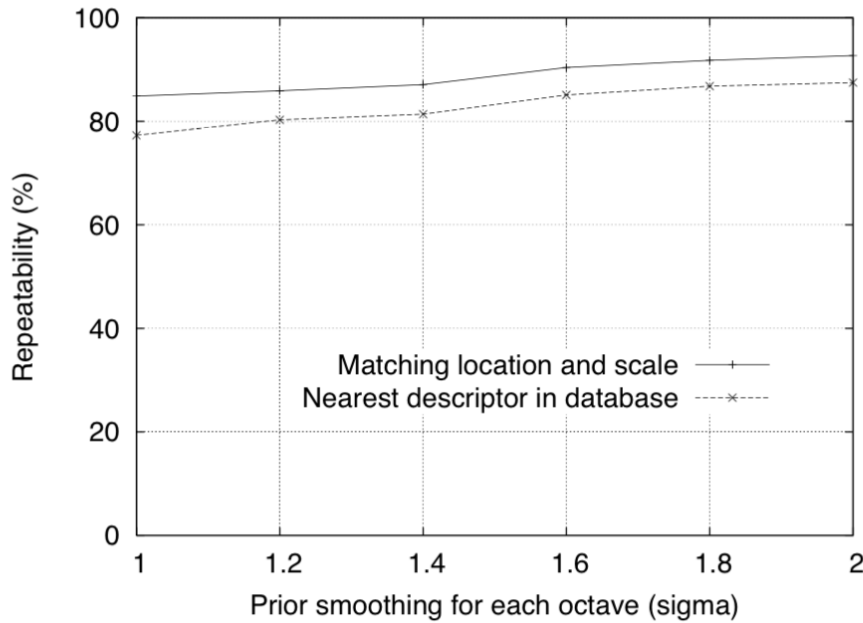


Figure 10. The top line shows the percent of keypoint locations that are repeatedly detected in transformed images as a function of the prior image smoothing for the first level of each octave. The lower line shows the percent of descriptors correctly matched against a large database. Reference [32]

$$D(\mathbf{x}) = D + \frac{\partial D^T}{\partial \mathbf{x}} \mathbf{x} + \frac{1}{2} \mathbf{x}^T \frac{\partial^2 D}{\partial \mathbf{x}^2} \mathbf{x}$$

Figure 11. Determine the interpolated location of the maximum. Reference [32]

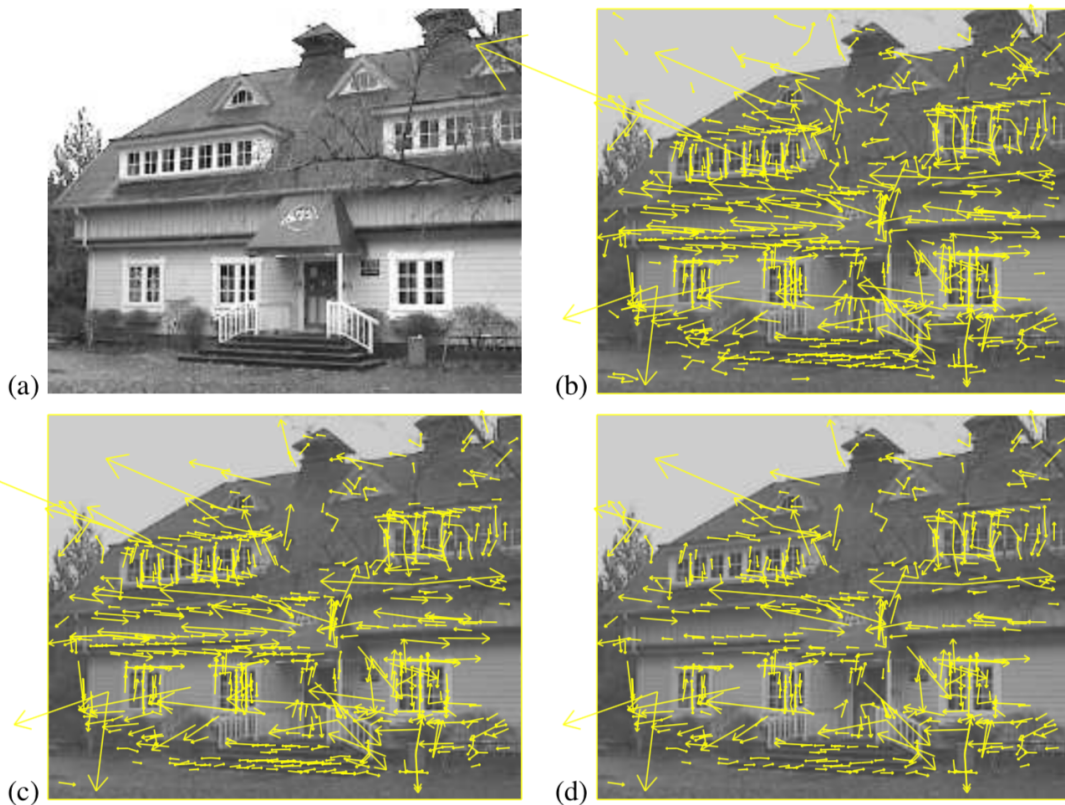


Figure 12. This figure shows the stages of keypoint selection. a) Original image b) initial keypoints location displayed as vectors c) threshold d) additional threshold applied on ratio of principal curvatures. Reference [32]

The location of extremum is determined by taking the derivate of this function,

$$\hat{\mathbf{x}} = -\frac{\partial^2 D}{\partial \mathbf{x}^2}^{-1} \frac{\partial D}{\partial \mathbf{x}}.$$

Figure 13. Function for derivate extremum. Reference [32]

Substituting in the above equation, the value obtained is useful for rejecting unstable extrema with low contrast.

$$D(\hat{\mathbf{x}}) = D + \frac{1}{2} \frac{\partial D^T}{\partial \mathbf{x}} \hat{\mathbf{x}}.$$

Figure 14. Function value at extremum. Reference [32]

2.1.2.1 Eliminating edge responses

For stability, rejecting keypoints with low contrast is not sufficient. Along the edges difference of Gaussian will have a strong response irrespective mismatch in the location.

A large curvature across the edge will have poor define peaks in the difference of Gaussian. There is a small one along the perpendicular direction which can be computed using a 2X2 Hessian matrix \mathbf{H} followed by eigenvalues.

$$\mathbf{H} = \begin{bmatrix} D_{xx} & D_{xy} \\ D_{xy} & D_{yy} \end{bmatrix}$$

$$\begin{aligned} \text{Tr}(\mathbf{H}) &= D_{xx} + D_{yy} = \alpha + \beta, \\ \text{Det}(\mathbf{H}) &= D_{xx}D_{yy} - (D_{xy})^2 = \alpha\beta. \end{aligned}$$

Figure 15. Hessian Matrix and eigenvalues. Reference [32]

For the principal curvature ratio to be less than the threshold r , we need to check

$$\frac{\text{Tr}(\mathbf{H})^2}{\text{Det}(\mathbf{H})} < \frac{(r+1)^2}{r}.$$

Figure 16. Function to check ratio of principal curvature is below threshold.

Reference [32]

2.1.3 Orientation assignment

For each image sample $L(x,y)$, at a particular pixel, the gradient magnitude $m(x,y)$ and orientation $\theta(x,y)$ is computed using pixel differences. Within the regions around the keypoints gradient orientation of sample points forms the histogram.

$$m(x,y) = \sqrt{(L(x+1,y) - L(x-1,y))^2 + (L(x,y+1) - L(x,y-1))^2}$$

$$\theta(x,y) = \tan^{-1}((L(x,y+1) - L(x,y-1))/(L(x+1,y) - L(x-1,y)))$$

Figure 17. Function to derive orientation histogram. Reference [32]

The dominant directions of local gradients correspond to the peaks in the orientation histogram. Experimental stability of location, scale and orientation assignment under differing amounts of noise in the image is shown in figure 18.

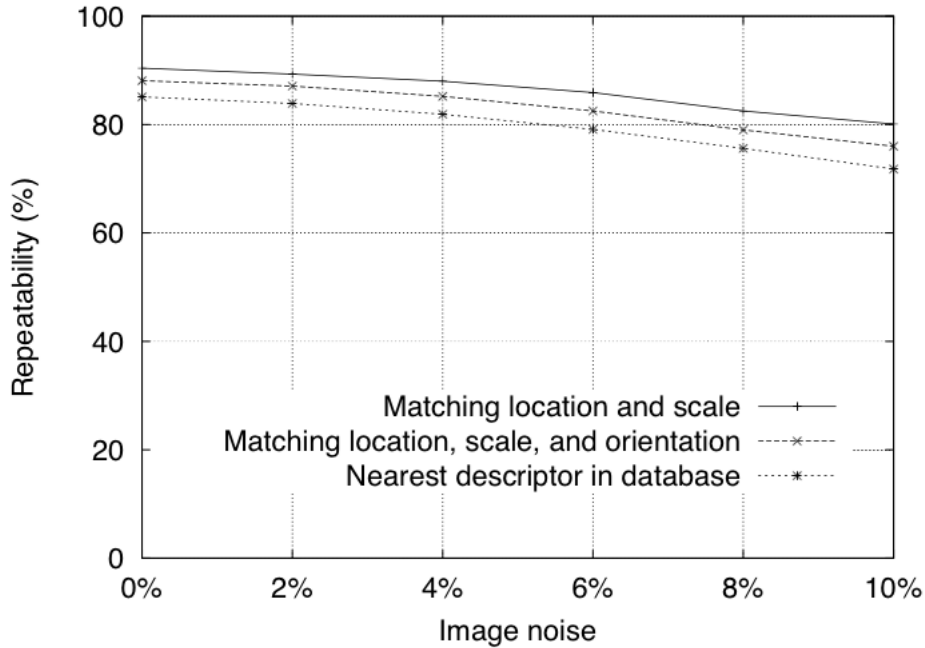


Figure 18. The top line shows percent of keypoints location that are repeatably detected as a function of pixel noise. The second line shows repeatability after also requiring agreement in orientation. The bottom line shows the final percent of descriptors correctly matched to a large database. Reference [32]

2.1.4 Keypoint Descriptor

Figure 19 illustrates the computation of the keypoint descriptor. To achieve orientation invariance, gradients are pre-computed in step 2.1.3 and are illustrated with small arrows on left side of the image.

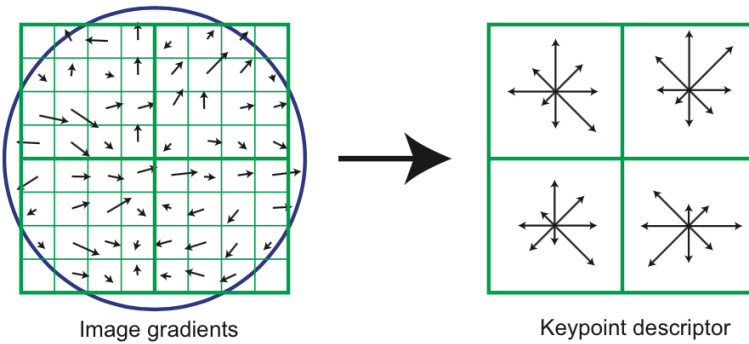


Figure 19. Showing the computed image gradients and keypoint descriptors.

Reference [32]

2.1.5 Keypoint Matching

The more effective way to match candidates is to compare the distance of the closest neighbor to the second closest neighbor. Figure 20 shows the importance of this value for real image data.

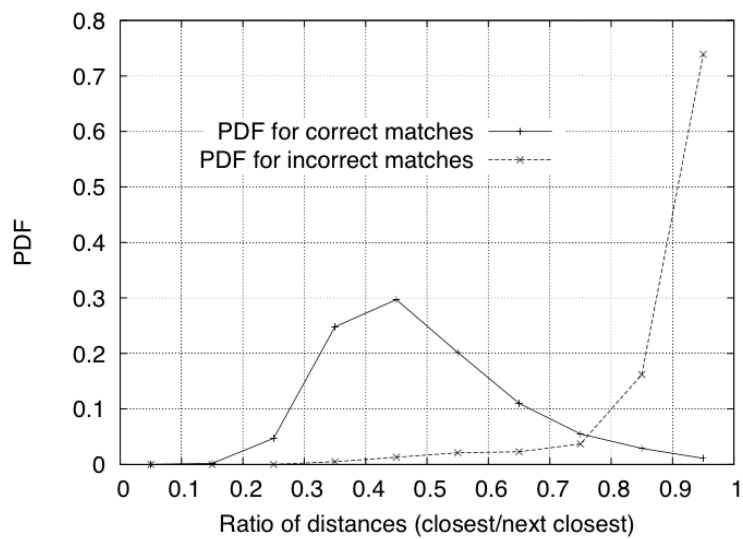


Figure 20. Show the probability of match. Reference [32]

This paper has implemented the least pose square estimation [41] to determine whether the reference image lies within the current image. The keypoint consists of four properties, scale, location, orientation and feature vector. Figure 21 shows the SIFT feature points and their match for three different face images.

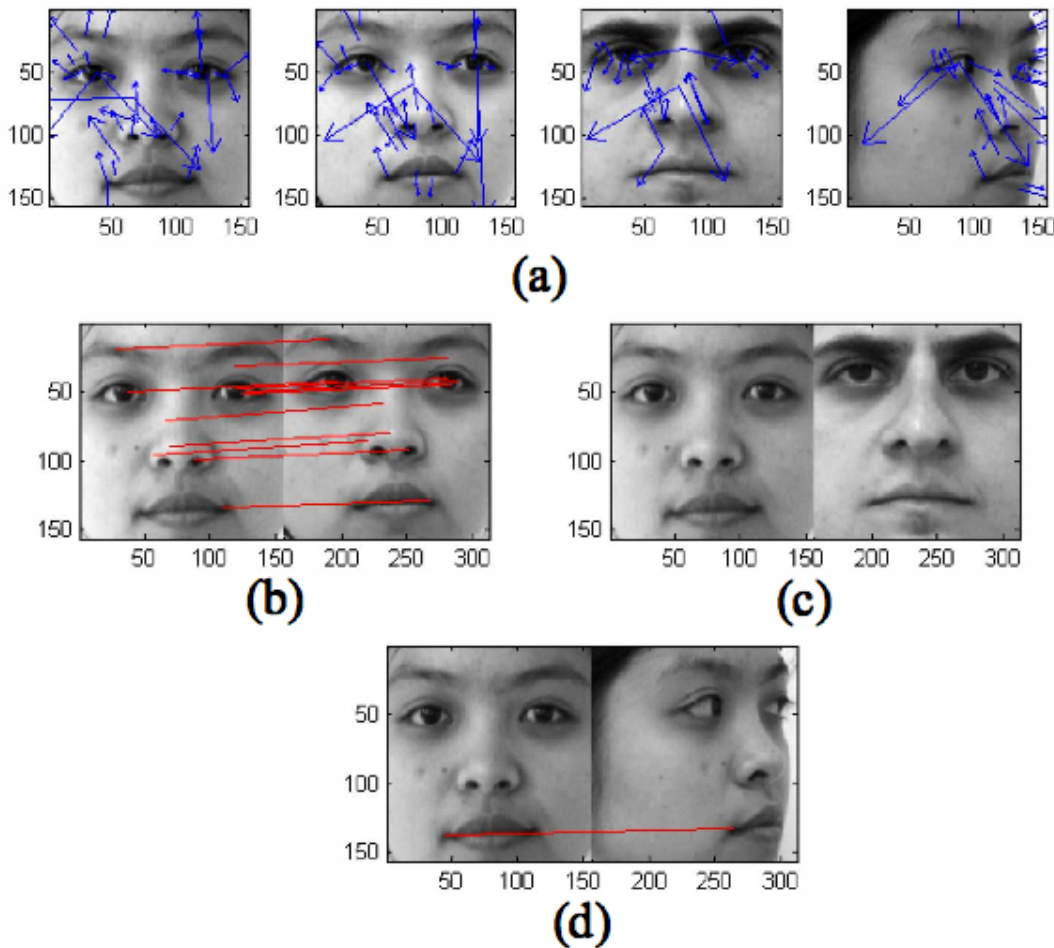


Figure 21. Sift features and their match of three face images. a) Images with SIFT feature b) Match of same face c) Match of different face d) Match of the same face with different poses. Reference [41]

The basic workflow for Scale Invariant Feature transform is shown in figure 22.

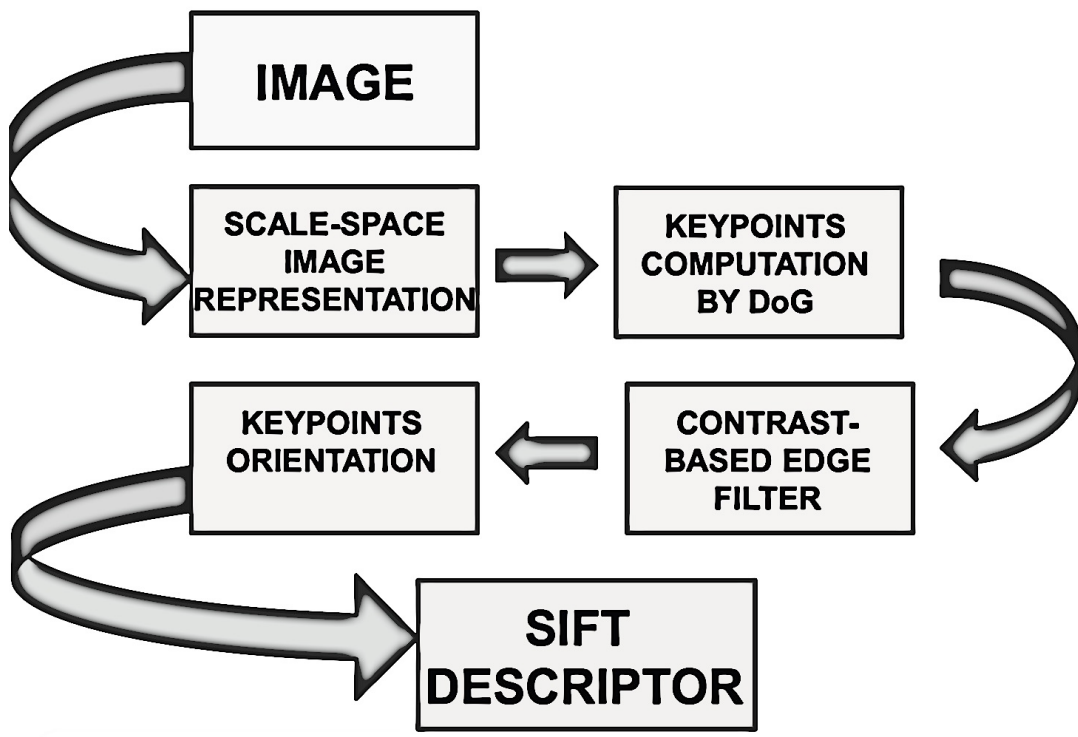


Figure 22. SIFT Workflow. Reference [42]

Chapter 3

Head Curve Geometry based Face Detection.

This thesis presents an enhanced method to segment face by implementing a lesser complex statistical approach called as the head curve geometry. Reason for choosing the thermal image is prominently due to its nature of not being prone to drastic ambient light changes and being statistically less complex. This section provides an insight for the basic setup for capturing and performing segmentation using the above-mentioned algorithm.

3.1 Image Segmentation

The salient image regions cluster the pixels i.e. regions corresponding to individual surfaces, objects, or natural part of objects. Also it has applications in object recognition, occlusion boundary estimation within motion or stereo systems, image compression, image editing etc. It also provides useful information about the surfaces in the scene. The methods vary from simple threshold to k-means clustering or Otsu's method, which prefers threshold to minimize intra class variance of the black and white pixels.

3.2 Setup

The initial setup for capturing the thermal images was carried out by Faculty of Engineering and Technology, Multimedia University (MMU), Melaka, Malaysia. The proposed system for face detection using a thermal imaging system is shown in figure 23. The experimental system comprises of a thermal camera, a computer installed with MATLAB and an appliance for further image processing.

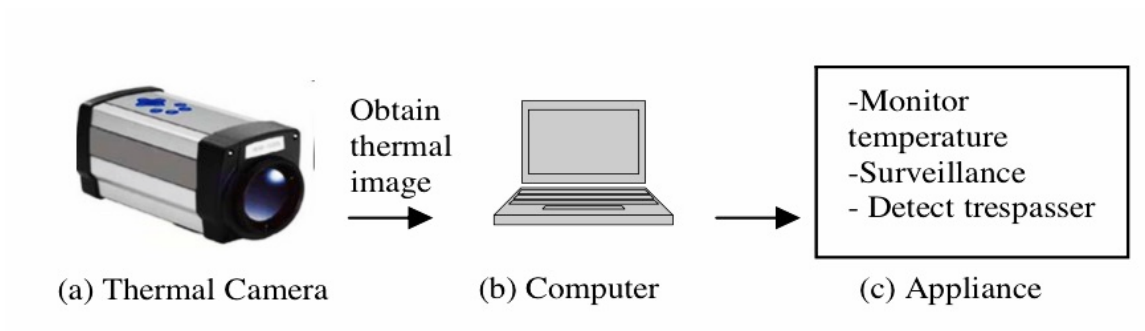


Figure 23. Thermal Imaging based Face Detection System. Reference [19]

3.2.1 Thermal Camera

The thermal camera deployed in this setup is Thermo Vision A-20M, produced by the FLIR system. The A20M has an advanced, uncooled micro bolometer FPA detector technology to deliver crisp, long wave images in a multitude of palates for temperature variations as low as 0.12°C . Real time acquisition at standard video rates (60 Hz) can reveal rapid, thermally transient events with clear

images. It also provides extensive connectivity options for digital output; one of them is FireWire (IEEE 1394a - standard for a serial bus for high-speed communication and isochronous real time data transfer). Also, it equips RJ-45 Ethernet ports as shown in Figure 24 that are ideal for individual or networked multiple camera installations.



Figure 24. Back Camera Interface FLIR Systems, Thermo Vision A-20 M [43]

3.2.2 Computer and appliance

The computer/laptop receives the detected thermal images for the thermal camera and processes them further using the MATLAB program. Once the face is extracted from an image, the output is sent to an appliance, such as the temperature monitoring system, tracking trespasser in the dark, and the surveillance system for further analysis. Figure 25 portrays the standard set up of the thermal camera at MMU.

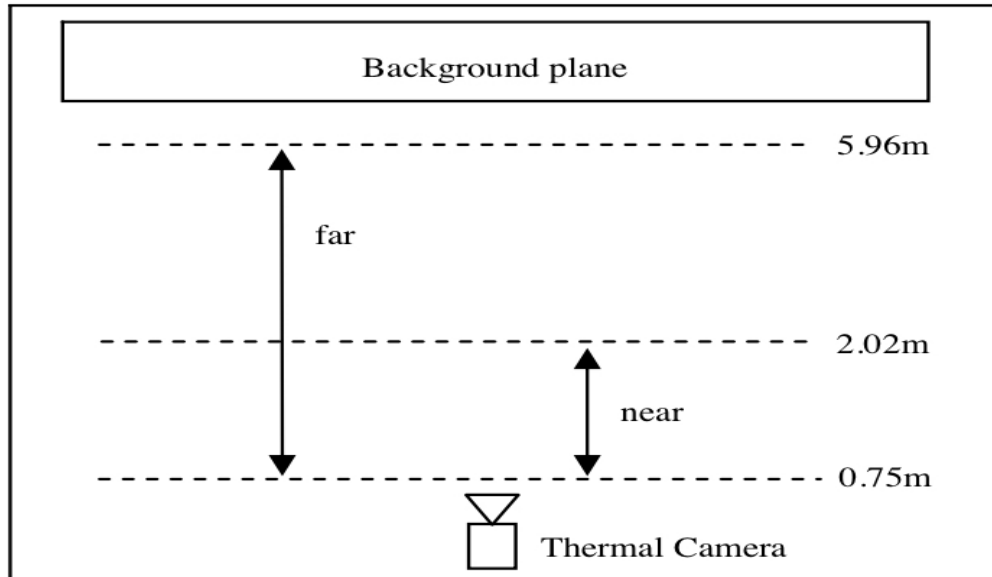


Figure 25. Experimental setup for thermal camera. Reference [19]

3.3 Head Curve Geometry Based Face Detection Algorithm

The face is extracted from the body after five points are located on the head boundary [44]. Head Point being the top-most point serves as the basis of search for other points on the boundary comprising of right most and left most points and neck points apart from the maximum mean points on the boundary. The curve is drawn around the neck region to separate out the desired face image. This algorithm has three main components, namely, Pre-Processing i.e. acquiring the thermal image and doing basic morphological operations. Second, searching for

points in the object boundary and lastly, draw curve to separate face from the input image.



Figure 26. Flowchart of proposed Head Curve Detection Algorithm.

3.3.1 Pre Processing

Pre-processing involves acquiring image and operating morphological operations such as erosion, closing, filling and boundary extraction. Threshold is also applied before the morphological operators to isolate the image from the background noise (separation of light and dark regions) and create the binary image. All the steps have been arranged from the first step as below.

Step 1: Acquire the thermal Image, thImg.

Step 2: As the above image is RGB image, extract the red component from the above input image output is imgRed.

Step 3: Apply threshold on the above extracted image.

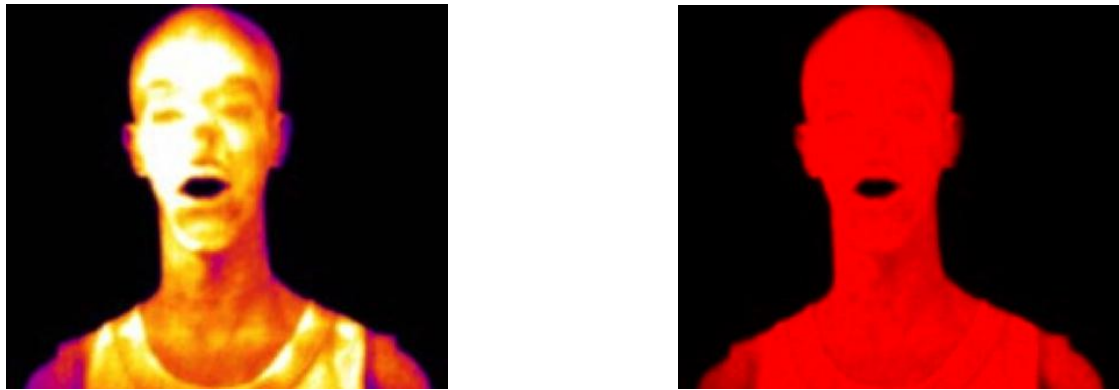


Figure 27. (a) RGB Image (b) Red component of RGB Image

Step 4: Convert imgRed into a black and white image, bwinRed.

$$\text{bwinRed}(m, n) = \begin{cases} 1, & \text{imgRed}(m, n) > \text{thImg} \\ 0, & \text{otherwise} \end{cases}$$

Where m,n are row and column matrix coordinate and thImg is the threshold value.

Step 5: Apply erosion (the basic effect of operator on the binary image is to erode away the boundaries of regions of foreground pixels i.e. white pixels). Generate a disk element, seM with radius rDisk.

Step 6: Perform morphological closing which is basically dilation followed by an erosion using the same structuring element for both operations on bwinRed. The output image is bwinClo.

Step 7: Generate another image bwinFil by filling the holes in bwinClo image.

Step 8: Save coordinate arrays for the obtained boundary image.



Figure 28. a) bwinRed b) bwinClo c) bwinFil

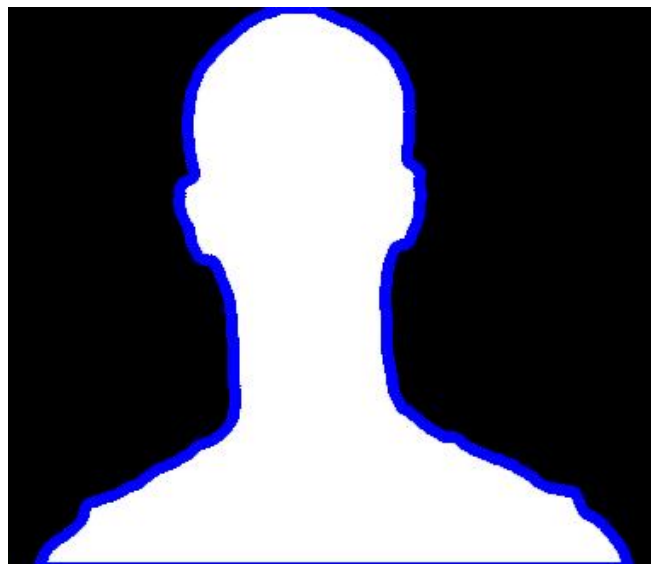


Figure 29. Image with extracted boundary

3.3.2 Searching for Points

This section covers the major steps involved in locating the appropriate points to define the curve to be drawn.

Step 1: From the extracted object boundary, find the mean x coordinate value and minimum y coordinate value.

Step 2: The highest point (minimum y coordinate) between the intersection points of the boundary and the vertical x mean point is the starting point i.e. the head top point (Head point). Refer to figure 30(a).

Step 3: Find the left and right mean points divide the previously extracted boundary in two parts left and right.

Step 4: Intersect the left & right pieces with the horizontal y line to find the respective left and right mean points. Refer to figure 30(b) (c).

Step 5: Find the left most mean point, traverse from the head point to the left mean point in counter clock wise direction to scout for the most left point by comparing the x (horizontal) coordinates.

Step 6: In the left boundary, the pixel with minimum x value corresponds to the most left point. Refer to figure 30(d).

Step 7: Find the right most mean point, traverse from the head point to the right mean point in counter clock wise direction to scout for the most right point by comparing the x (horizontal) coordinates.

Step 8: In the right boundary, the pixel with maximum x value corresponds to the most right point. Refer to figure 30(e).

Step 9: Optionally, Distance from Head Point between left most & right most points can be calculated using distance2curve function.

Step 10: To find the right neck point traverse in clockwise direction from right most point to the right mean point and extract the boundary coordinate points.

Step 11: From the boundary points, the pixel with minimum x value will be the left neck point. Refer to figure 30(f).

Step 12: To find the left neck point traverse in the clockwise direction from the left most point to the left mean point. Extract the coordinate points from the boundary.

Step 13: From the boundary points, the pixel with maximum x value will be the right neck point. Refer to figure 31(g).

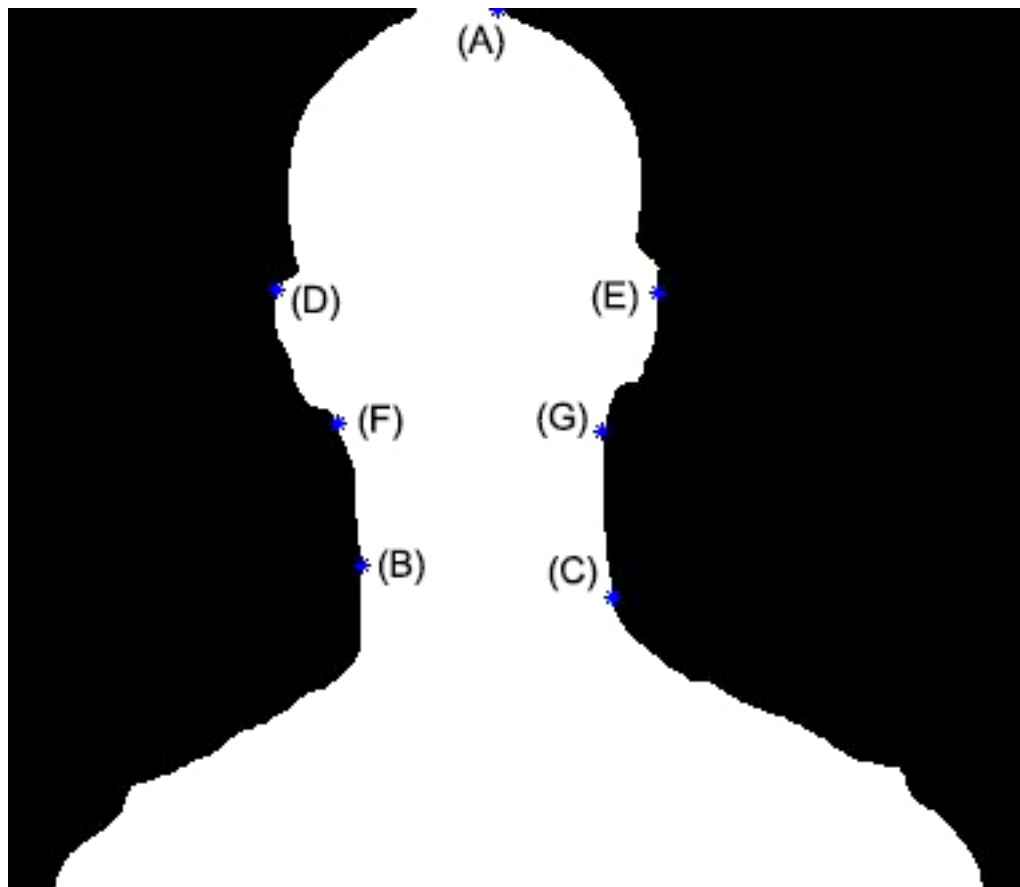


Figure 30. Shows the following points: a) Head point b) Left Mean Point c) Right Mean Point d) Left Most Point e) Right Most Point f) Left Neck Point g) Right Neck Point

3.3.3 Drawing Curve for face extraction

When all required points have been found in the head boundary, we find the center point to draw the radius for separating the image in two parts where the head point in the boundary will be the required face image.

Step 1: Determine the center point, cendraw for the curve, using the x and y coordinates from the left most and the right most points.

Step 2: The Average of the y coordinates from both the points will yield y coordinate of the cendraw i.e. cendrawY.

Step 3: Locate the two points (point A and point B) by extending the horizontal y-axis at the value of cendrawY across the head boundary.

Step 4: Calculate the average of above two points to determine x coordinate of cendraw i.e. cendarwX.

Step 5: Measure distance from both point A and point B to cendraw. The maximum value between two measured distances will be the radius to curve to be drawn.

Step 6: From the center point, cendraw and calculated radius plot the curve on the head boundary. Refer to figure 31.

Step 7: Create a facemask to separate the two images into two different images for extracting face, the desired output. The final image is shown in the figure 32.

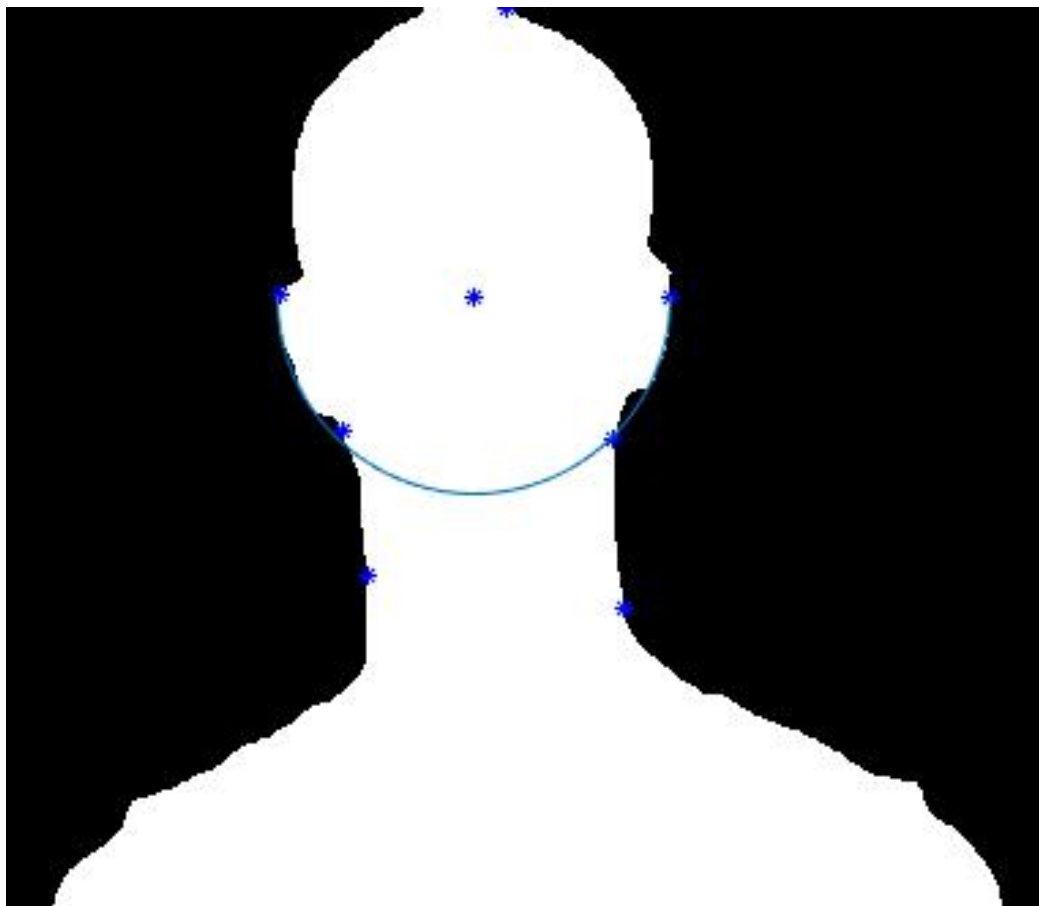


Figure 31. Shows the curve plot on the head boundary.

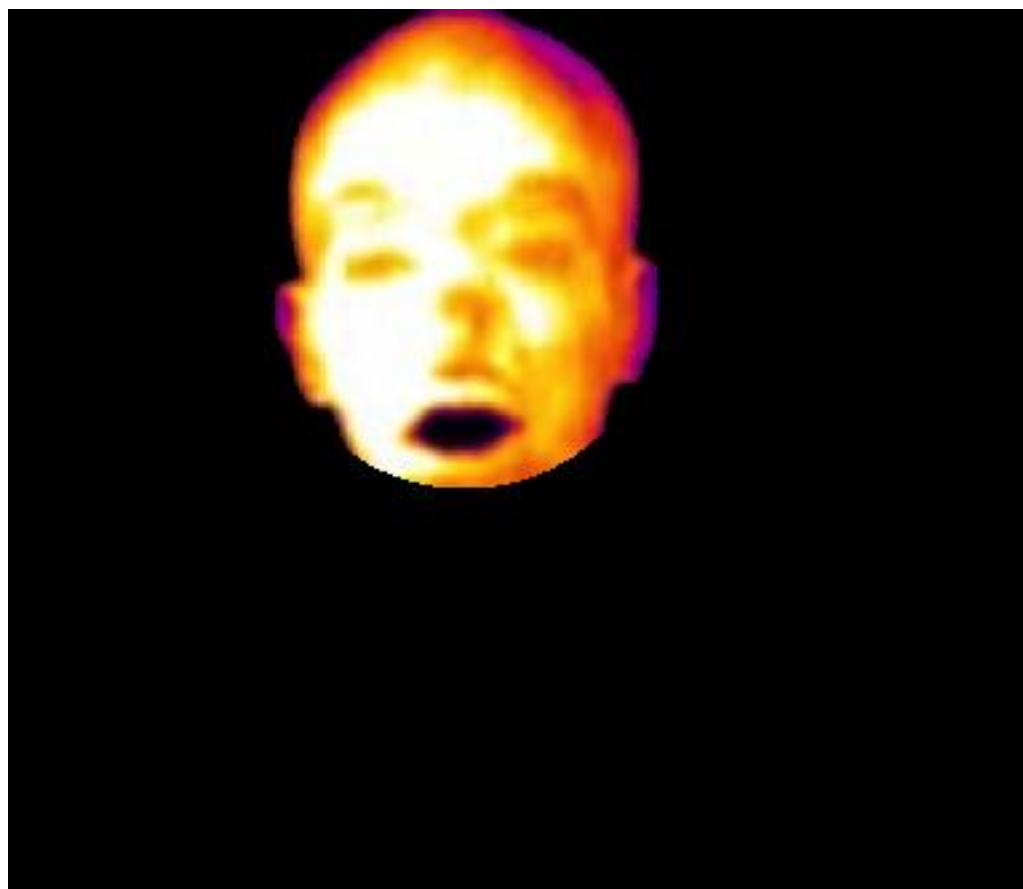


Figure 32. Shows face separated using the head curve geometry.

Chapter 4

Image Matching using Scale Invariant Feature Transform

After retrieval of face from the source image using the head curve geometry, Scale Invariant Feature Transform is exercised to locate the reference image within the current image. This process uses subset of the image for reference and applies transformation

The Important steps implemented are:

Step 1: Get the Image data. This paper has used the subset approach i.e. subset of the image from the reference image is extracted3.

Step 2: Get feature points. This has been implemented using David Lowe approach discussed earlier in Chapter 2. It also implements affine invariance [45] that approximates viewpoint changes for roughly planar objects and roughly orthographic cameras.

Step 3: Get descriptors. Calculate the sift vectors from sift patches for each possible orientation.

Step 4: Get the match points. This static method matches the feature points that have similar sift vectors.

Step 5: Get pose. This static method performs the least square pose estimation based on the matched point.

Step 6: Gaussian pyramid is implemented for current and reference images to create a series of images, which are oppressed using Gaussian average (blur).

4.1 Experimental Results

The test image is the subset of the reference image. Transformation is applied on the reference image to locate the reference image in the current image. The following images list the results from the applied algorithm.

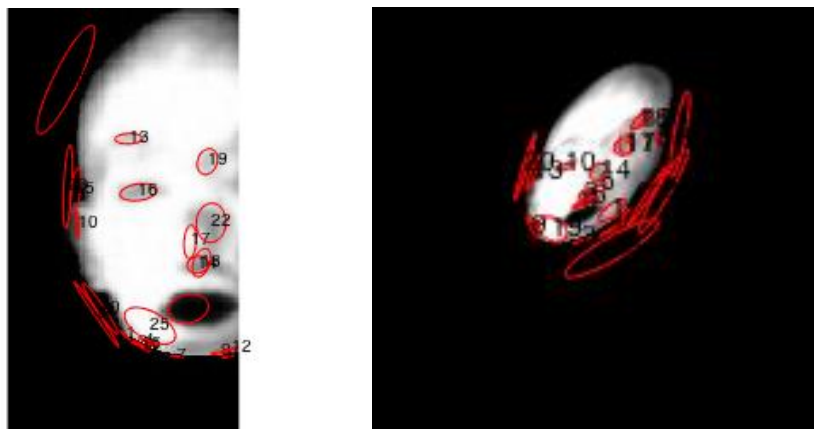


Figure 33. a) Reference Image b) Image with descriptors

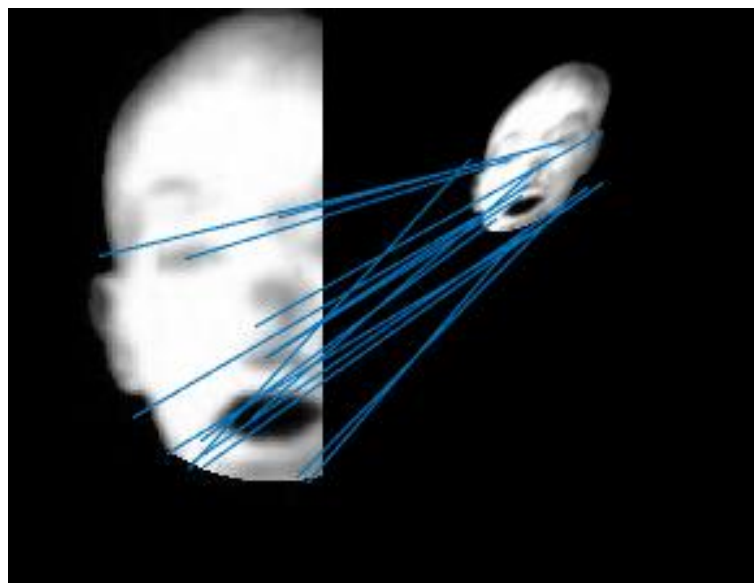


Figure 34. Showing the Matched points in reference image.

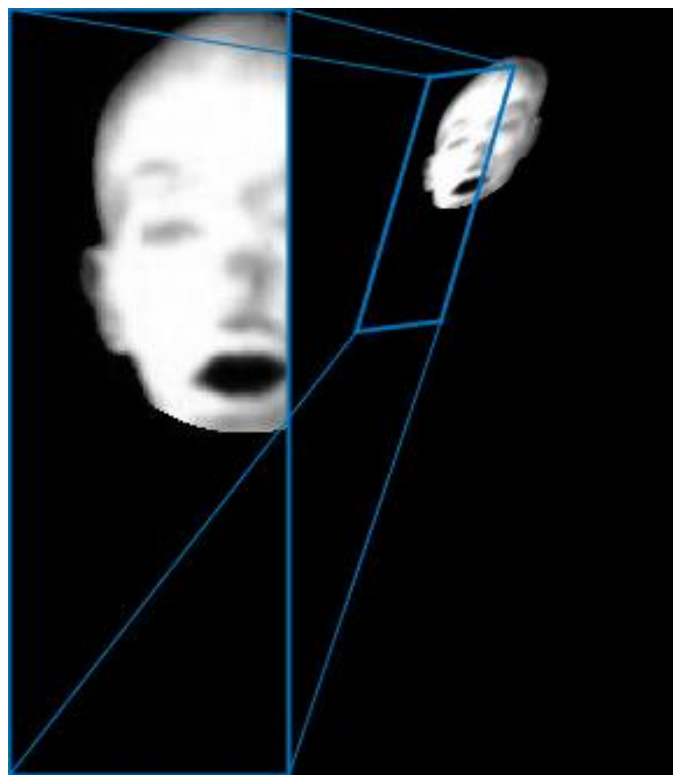


Figure 35. Showing the Pose estimation.

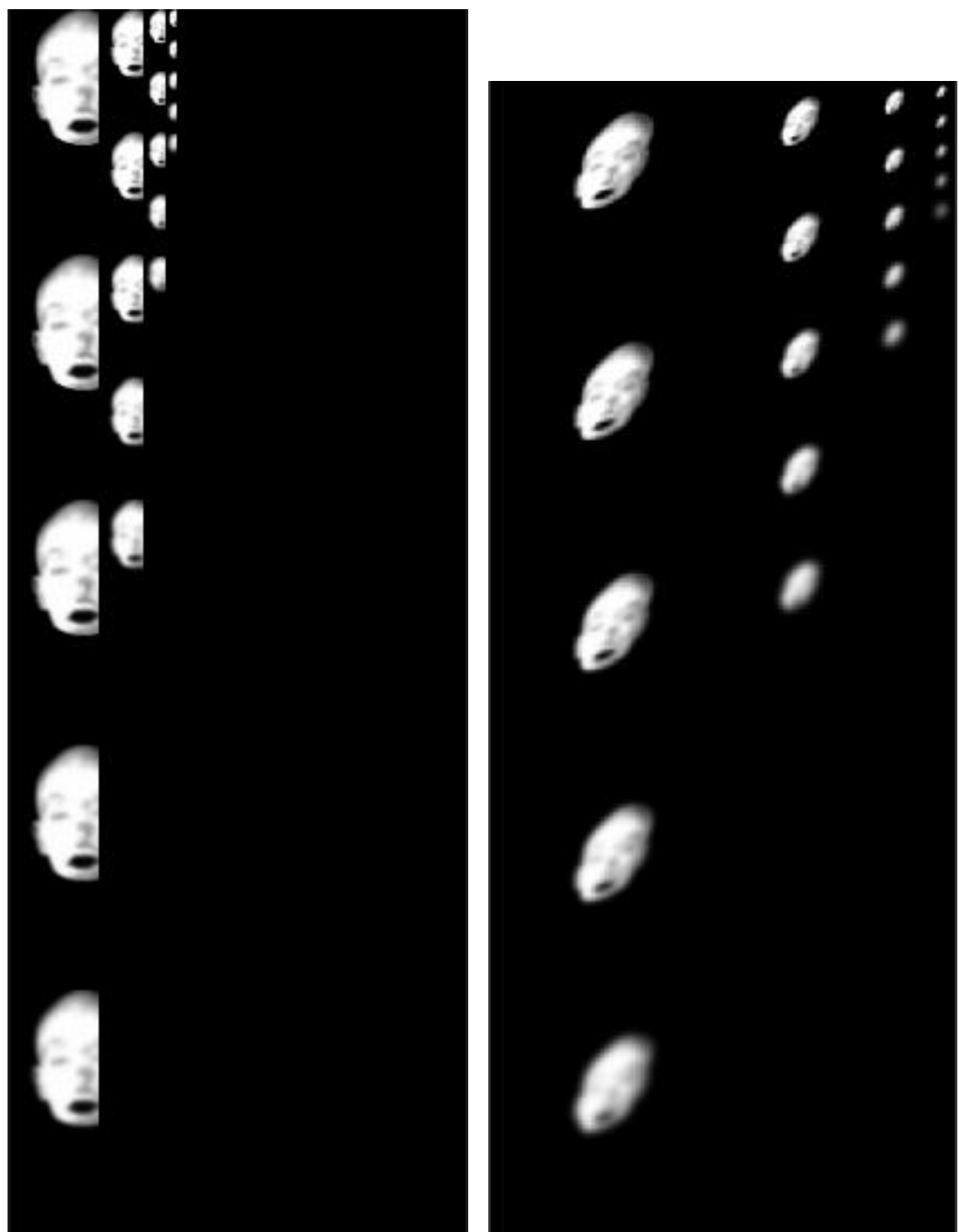


Figure 36. Pyramid plots for a) reference and b) current Image

Chapter 5

Conclusion & Future Scope

Face being an important biometric identifier has received an ardent following in recent times and move from visual band to infrared band has given researchers a platform to dwell on unlimited possibilities for better security and privacy related to important issues like Banking, Homeland Security etc. The near infrared images add a new dimension to recognize face by separating illuminated faces under varying ambient illumination with ease [29].

In Head Curve Geometry, rDisk the radius size to plot a disk shaped structuring element for the morphological process in Chapter 3, plays an important role in defining the neighborhood boundaries. A larger value might lead to a bigger blob in image resulting in an erroneous output or miss alignment of points on the image with respect to the boundary.

Scale Invariant Feature Transform does recognize objects in unknown configurations; to identify keylocation in scale space is a concern as of background noise or undetected feature in training images. However, the object model can undergo limited affine projection, planar shapes can be recognized at

60 degrees rotation away from the camera and individual features can be matched to a large set of an object database.

Face recognition in thermal images using head curve geometry in the future may be applied for variant poses and delineated face from the rest of the body, helps carry out the segmentation of superficial blood vessels from facial tissue [46]. This can be used to infer the body temperature or any psychological conditions one is going through. Since head curve geometry has minimum processing time comparing to other complex algorithms, in future more images with more pose differences will help create a pose estimation database at faster pace for unlimited possibilities.

References

- [1] Jain, Anil K., Ross, Arun A., Nandakumar, Karthik., "Introduction to Biometrics" © Springer Science + Business Media, LLC 2011), DOI 10.1007/978-0-387-77326-1_1.
- [2] Jain, A., Hong, L., & Pankanti, S. (2000). "Biometric Identification" Communications of the ACM, 43(2), p. 91-98. DOI 10.1145/328236.328110
- [3] W. Zhao, R. Chellappa, P.J. Phillips, and A. Rosenfeld, "Face Recognition: A Literature Survey" ACM Computing Surveys, vol. 35, no. 4, pp. 399-458, Dec. 2003
- [4] Y. Adini, Y. Moses, and S. Ullman, "Face Recognition: The Problem of Compensating for Changes in Illumination Direction" IEEE Trans. Pattern Analysis and Machine Intelligence, vol. 19, no. 7, pp. 721-732, July 1997.
- [5] I. Pavlidis and P. Symosek, "The Imaging Issue in an Automatic Face/Disguise Detection System" IEEE Workshop Computer Vision Beyond the Visible Spectrum: Methods and Applications, pp. 15- 24, June 2000.

- [6] S.Z. Li, L. Zhang, S. Liao, X. Zhu, R. Chu, M. Ao, and R. He, "A Near-Infrared Image Based Face Recognition System" Seventh Int'l Conf. Automatic Face Gesture Recognition, pp. 455-460, 2006.
- [7] F. Prokoski, "History, Current Status, and Future of Infrared Identification" IEEE Workshop Computer Vision beyond the Visible Spectrum: Methods and Applications, pp. 5-14, June 2000.
- [8] D.A. Socolinsky and A. Selinger, "A Comparative Analysis of Face Recognition Performance with Visible and Thermal Infrared Imagery" Sixteenth International Conference on Pattern Recognition, vol. 4, pp. 217-222, 2002.
- [9] D.A. Socolinsky, L.B. Wolff, J.D. Neuheisel, and C.K. Eveland, "Illumination Invariant Face Recognition Using Thermal Infrared Imagery" IEEE CS Conf. Computer Vision and Pattern Recognition, vol 1, pp. 527-534, 2001.
- [10] A. Selinger and D.A. Socolinsky, "Face Recognition in the Dark", Proc. Joint IEEE Workshop Object Tracking and Classification beyond the Visible Spectrum, June 2004.

- [11] X. Chen, P.J. Flynn, and K.W. Bowyer, "PCA-Based Face Recognition in Infrared Imagery: Baseline and Comparative Studies" IEEE Int'l Workshop Analysis and Modeling of Faces and Gestures, pp. 127-134, Oct 2003.
- [12] P. Buddharaju, I. Pavlidis, and I. Kakadiaris, "Face Recognition in the Thermal Infrared Spectrum" Joint IEEE Workshop Object Tracking and Classification beyond the Visible Spectrum, June 2004.
- [13] J. Heo, S.G. Kong, B.R. Abidi, and M.A. Abidi, "Fusion of Visual and Thermal Signatures with Eyeglass Removal for Robust Face Recognition" Joint IEEE Workshop Object Tracking and Classification beyond the Visible Spectrum, June 2004.
- [14] A. Gyaourova, G. Bebis, and I. Pavlidis, "Fusion of Infrared and Visible Images for Face Recognition" Proc. Eighth European Conf. Computer Vision, May 2004.
- [15] S.G. Kong, J. Heo, B.R. Abidi, J. Paik, and M.A. Abidi, "Recent Advances in Visual and Infrared Face Recognition—A Review" Computer Vision and Image Understanding, vol. 97, no. 1, pp. 103- 135, Jan. 2005.

[16] Anchit A., Mathur S., "Comparative analysis of Haar and Skin Color method for face detection" Recent Advances and Innovations in Engineering, pp 1-5, May 2014.

[17] Y. Li, S. Gong, J. Sherrah, and H. Liddell, "Support Vector Machine Based Multi-View Face Detection and Recognition" Image and Vision Computing, vol. 22, no. 5, pp. 413-427, 2004.

[18] Nazeer, S.A., Omar, N., Khalid, M., "Face Recognition System using Artificial Neural Networks Approach", Proc. International Conference on Signal Processing, Communications and Networking, pp 420-425, Feb 2007.

[19] Wong, Wai Kit., Hui, Joe How., Desa, Jalil Bin Md., Ishak, Nur Izzati Nadiah Binti., "Face detection in thermal imaging using head curve geometry" Fifth International Congress on Image and Signal Processing, pp 881-884, Oct 2012.

[20] Cong, Ceng., Xudong, Jiang., "SIFT features for face recognition" Second IEEE International Conference on Computer Science and Information Technology, pp 598-603, Aug 2009.

[21] B. Bates, "A Guide to Physical Examination and History Taking" Fifth ed. Philadelphia, PA: Lippincott, p.181-215, 1991.

- [22] W. Zhao, R. Chellappa, P. Phillips, and A. Rosenfeld, "Face Recognition: A Literature Survey" ACM Computing Surveys, pp. 399-458, 2003.
- [23] M.A. Turk and A.P. Pentland, "Eigenfaces for Recognition" J. Cognitive Neuroscience, vol. 3, no. 1, pp. 71-86, Mar. 1991.
- [24] Bowyer, K.W., "Face recognition technology: security versus privacy" IEEE Technology and Society magazine, vol 23, issue 1, pp 9-19, Spring 2004.
- [25] K. Chang, K. Bowyer, S. Sarkar, and B.Victor, "Comparison and combination of ear and face images for appearance-based biometrics" IEEE Trans. Pattern Analysis and Machine Intelligence, vol. 25, no.9, pp.1160 - 1165, Sept. 2003
- [26] J. Phillips, S. Sarkar, I. Robledo, P.Grother, and K.W. Bowyer, "Baseline results for the challenge problem of Human ID using gait analysis" in Proc. Face and Gesture Recognition 2002, Washington, DC, pp 137-142.
- [27] F. Prokoski, "History, Current Status, and Future of Infrared Identification" Proc. IEEE Workshop Computer Vision beyond the Visible Spectrum: Methods and Applications, pp. 5-14, June 2000.

- [28] Manohar, "Extraction of Superficial Vasculature in Thermal Imaging" master's thesis, Dept. Electrical Eng., Univ. of Houston, Houston, Texas, Dec 2004.
- [29] Stan Z. Li, RuFeng Chu, ShengCai Lao, Lun Zhang, "Illumination invariant face recognition using near infrared images" IEEE transaction on pattern analysis and machine intelligence, Vol 29. , No. 4., April 2007.
- [30] B.J. Moxham, C. Kirsh, B. Berkovitz, G. Alusi, and T. Cheeseman, Interactive Head and Neck (CD-ROM). Primal Pictures, Dec. 2002
- [31] Guohua Yue, Yu Xu, "An area based Image Matching Algorithm and it's implementation" Third World Congress on Software Engineering, pp 147-150. 2012.
- [32] Junlop, J.D., Holder, G.H., LeDrew E.F., "Geoscience and Remote Sensing Symposium 1989. 12th Canadian Symposium on Remote Sensing", Volume 3, pp 1273-1276, Jul 1989.
- [33] D.Lowe, "Distinctive Image Features from Scale-Invariant Keypoints" Intl. Journal of Computer Vision, Vol.2, No. 60, pp 91-110, 2004.

- [34] C. Xiaochun, H. Yihua, H. Gulan, T. Xiaohong, and L. Wuhu, "Morphology based adaptive preprocessing method of infrared image sequence" SPIE 27th Int. Congress on High-Speed Photography and Photonics6279, 62793C-6 (2007).
- [35] P. Soille, "Morphological image analysis-principle and applications", © Springer, Germany, 1999.
- [36] Rafael C. Gonzalez, Richard E. Woods, "Digital Image Processing" Third Edition, Pearson, ISBN 978-81-317-1934-3.
- [37] Duda, R. O. and P. E. Hart, "Use of the Hough Transformation to Detect Lines and Curves in Pictures" *Comm. ACM*, Vol. 15, pp. 11–15 (January, 1972).
- [38] Andrew P. Witkin, "Scale-space filtering", Proceedings of the Eight international joint conference on artificial intelligence" Vol. 2, pp 1019-1022, 1983.
- [39] Lindeberg, T. 1993. "Detecting salient blob-like image structures and their scales with a scale-space primal sketch: a method for focus-of-attention" International Journal of Computer Vision, 11(3): 283-318.

[40] Brown, M. and Lowe, D.G. 2002. "Invariant features from interest point groups" In British Machine Vision Conference, Cardiff, Wales, pp. 656-665.

[41] Xian Bing, Juan Wu, Xin Zhang, Long Zhang, Sheng Zhan, " A novel multi pose face recognition via robust SIFT feature" Int. Conf. on Wavelet Analysis and Pattern Recognition, pp. 23-37, 2013.

[42] <https://copilosk.fbk.eu/images/f/f6/Sift.pdf>

[43] <http://alacron.com/clientuploads/directory/Cameras/FLIR/A20M-Datasheet.pdf>

[44] Wai Kit Wong, Joe How Hui, Chu Kiong Loo and Way Soong Lim, "Off-time Swimming Pool Surveillance Using Thermal Imaging System" 2011 IEEE International Conference on Signal and Image Processing Applications (ICSIPA11), p 366 – 371.

[45] http://web.engr.illinois.edu/~slazebni/spring11/lec08_blob.pdf

[46] C. Manohar, "Extraction of Superficial Vasculature in Thermal Imaging" master's thesis, Dept. Electrical Eng., Univ. of Houston, Houston, Texas, Dec 2004.